# An Emergency Active and Reactive Power Exchange Solution for Interconnected Microgrids

Mobin Naderi; Yousef Khayat; Qobad Shafiee; Tomislav Dragicevic; Frede Blaabjerg, Hassan Bevrani

Published (to be published) in: ***IEEE Journal of Emerging and Selected Topics in Power Electronics***

(Expected) publication date: **2019**

**Citation format for published version:**

Mobin Naderi; Yousef Khayat; Qobad Shafiee; Tomislav Dragicevic; Frede Blaabjerg, Hassan Bevrani. (2019, November 19). An Emergency Active and Reactive Power Exchange Solution for Interconnected Microgrids. *IEEE Journal of Emerging and Selected Topics in Power Electronics*(2168-6777), 1-1. doi:10.1109/JESTPE.2019.2954113

This article has been accepted for publication in a future issue of this journal, but has not been fully edited. Content may change prior to final publication. Citation information: DOI 10.1109/JESTPE.2019.2954113, IEEE Journal of Emerging and Selected Topics in Power Electronics

# An Emergency Active and Reactive Power Exchange Solution for Interconnected Microgrids

Mobin Naderi, *Student Member, IEEE,* Yousef Khayat, *Student Member, IEEE,* Qobad Shafiee, *Senior Member, IEEE,* Tomislav Dragicevic, *Senior Member, IEEE,* Frede Blaabjerg, *Fellow, IEEE,* and Hassan Bevrani, *Senior Member, IEEE*

***Abstract*—In this paper, an important application of interconnected microgrids (IMGs) is presented in order to handle an emergency condition of individual microgrids (MGs), which causes an intolerable voltage magnitude or frequency deviation. In this method, the active and reactive powers are exchanged via an interlinking back-to-back converter (BTBC) and in accordance with voltage magnitude and/or frequency differences of individual MGs. In order to increase the IMG reliability and overcome the communication challenges, only local voltages and frequencies of both AC sides of the BTBC are used to determine the required active and reactive powers to be exchanged. A generalized droop control is employed to consider the impact of voltage magnitude and frequency differences on exchanging active and reactive powers separately for any type of interlinking lines. In this emergency power exchange method, a logical control is employed to detect the emergency and the normal conditions. The former results in the IMG formation, while the latter form the individual MGs operation again. The real-time results, obtained from OPAL-RT simulator, practically show advantages of the proposed method including voltage and frequency supports, postponing the load shedding, plug-and-play capability, good power sharing between the IMGs and method compatibility with the controls of individual MGs.**

***Index Terms*—Back-to-back converter, emergency control, generalized droop control, Interconnected microgrids, power exchange.**

## I. Introduction

MICROGRIDS are very well-known nowadays in the power industry. Their grid-connected and islanded operation modes present considerable capabilities such as reliability and power quality improvements, more flexible power production and increase of distributed generation (DG) penetration. Another operation mode of microgrids (MGs), which is less taken into account, is interconnected MGs (IMGs). In this operation mode, MGs can be interconnected with each other when they are islanded/connected from/to the grid. In both conditions, Interconnecting the MGs have much advantages such as reliability and resiliency improvement, penetration increase of DGs than individual MGs, load supply and unit generation flexibility, and improved load shedding after an emergency condition. These benefits are highlighted in the mode of islanded IMGs [1], [2]. An emergency condition that leads to enable load shedding control in an islanded MG can be supported by a power exchange in the IMG mode to postpone or even cancel the load shedding procedure.

IMG operation mode is usually an ancillary mode for individual islanded MGs or a distribution system. Going from each of these situations to the IMG mode can be planed or emergency-based (unplanned). It is worth to mention that in the planned IMG formation, Interlinking number of MGs is favorable in order to increase flexibility and reliability. However, for the emergency-based formation, interconnecting should be minimized despite available inactive interconnections in order to avoid propagation of probable instability.

The planned IMG formation, control and operation are mostly related to energy/power management level, which is done by a global MG control layer or distribution system operator (market operator) [3]–[6]. Nevertheless, low-level control characteristics such as voltage and frequency dynamics are taken into account in the literature [7]–[10]. Generally, the conventional secondary control-based power flow between multi-area power systems is developed for IMG power exchange through circuit breakers (CB).

Although, power exchange among areas of conventional power systems is a well-known function of the secondary control [11], [12], its application for CB-IMGs is still challenging issue due to intense interaction between the voltage and frequency, which is due to the weakness of AC voltage source converter (VSC)-based MGs. In [7], a special structure of AC MGs including PQ-controlled and droop-based DGs is considered in which the PQ-controlled DGs facilitate IMG power exchange, thus the challenges of fully droop-based MGs do not reveal. In [8], a conventional secondary control is proposed for CB-IMGs, but it is verified only for a small-signal model of the IMGs. The hierarchical control introduced in [9] is a power sharing method to supply common IMG loads that is not able to exchange power between IMGs. In [10], a distributed secondary control is developed that supports power exchange between CB-IMGs only for planned operations. None of the secondary control-based methods support emergency detection and unplanned IMG formation.

The emergency condition in an islanded MG is defined as large and sudden disturbances such as large load change or DG trip, which change the balance between generation and consumption [13]. The emergency-based IMG formation is determined usually due to such an emergency condition in a remote MG in order to support frequency and delay load shedding mechanisms [14]. It is also an alternative solution to using energy storage systems and extra-sized diesel generators [15], which can be more flexible.

IMGs can be classified based on MG or interlinking device type [16]. According to MG type, there are three IMG categories comprising fully AC IMGs [8], [10], [14], [17]–[19], fully DC IMGs [20], and hybrid AC-DC IMGs [21]–[23].

This article has been accepted for publication in a future issue of this journal, but has not been fully edited. Content may change prior to final publication. Citation information: DOI 10.1109/JESTPE.2019.2954113, IEEE Journal of Emerging and Selected Topics in Power Electronics

According to interlinking device type for AC IMGs, CBs and static switches can interconnect only MGs with same nominal voltages and frequencies [8]–[10], [14], however back-to-back converters (BTBCs) eliminate this limitation [17], [24], [25]. On the other hand, CBs are more reliable and economic for IMG formation, but BTBCs are more flexible. Frequency isolation is a remarkable advantage of BTBC-IMGs, specially paying attention to the low-frequency oscillations, which are appeared in CB-IMGs due to inter-microgrid interactions and may cause wide instability [8], [26].

In the literature of IMG control methods, a hierarchical frequency control is firstly proposed, which is fully based on the communication [27]. It is modified for DC MG clusters [20], AC and DC IMGs with one point of common coupling (PCC) [28], and fully AC IMGs [29]. In [20], the power sharing among DC MGs is based on the distributed consensus-based control, which reduces the communication infrastructure. However, the emergency detection is not included. In [28], a high-bandwidth communication is used only for power exchange without detection. Although the detection procedure is only included in [29], it requires a high-bandwidth communication. Furthermore, a different hierarchical control is recently introduced [9], which is widely communication-based and needs the information of spare powers and PCC voltages.

Some authors have researched on the control of an interlinking AC-DC converter of hybrid AC-DC MGs in order to share power properly [22], [23], [30]. In these hybrid MGs, power sharing is done only between two interconnected AC and DC MGs. A larger hybrid MG is investigated in [21], where two AC MGs and two DC MGs are interlinked using three AC-DC converters and without any need to BTBCs. The paper uses an event-based distributed control to share the power between the MGs while the communication and computational burden is reduced. Another distributed control is used in [17] for power sharing among fully AC IMGs. Power sharing is only based on the frequency differences of MGs, which is supported by ESS/STATCOM units in individual MGs. In [31], a parallel operation of HVAC and diode-rectifier HVDC links for offshore wind farms is investigated, which a composition of distributed and centralized controllers is employed to flow the generated wind power.

Communication-free methods are also proposed by employing modified droop controllers in order to exchange power among AC IMGs [19], [24], [32], [33]. All these papers present the IMG power exchange by controlling the inter-tied BTBC and only using the frequency deviations. In addition, no solution presents for seamless connection/disconnection of IMGs during/after an emergency control. Emergency-based IMG formation/cancellation has been presented in [14], [34], but only applicable for MGs with the same nominal voltages and frequencies due to using static switches instead of BTBCs.

### A. Summary of Power Exchange Methods

The power exchange methods among IMGs have been reviewed, which can be considered from different points of view. The power can be exchanged as planned [3]–[10] or emergency [14], [34]. In the planned type, the operator tries to find an economic solution to distribute power among IMGs for hours. However, the techniques are not fast enough to be used in the emergency condition. In contrast, the emergency power exchanges are not necessary to be economic, nevertheless they need to rescue the critical MG(s) in short critical time spans. Therefore, they should quickly be done like other emergency reactions, e.g. load shedding.

In terms of interlinking devices, the power exchange methods can be divided into two categories: 1) uniform-frequency IMGs through CBs [7]–[10] or instantaneous static switches [14], briefly named CB-IMGs, and 2) multi-frequency IMGs using BTBCs for AC IMGs [17], [24], [25], [32], [33] (BTBC-IMGs) or other power converter kinds for other IMG types [21]–[23], [28], [30]. The first group makes the interlinking hardware more economic. Nevertheless, it is limited to interconnect MGs with the same nominal frequencies in which the secondary controllers of droop-based DGs play the main role in exchanging power. Such a limitation is removed in BTBC-IMGs, while they are relatively expensive. Moreover, BTBC-IMGs benefit from more flexible control due to employing controllable power converters instead of CBs.

The level of using communication causes three different power exchange categories. Communication-based central controller is the first technology [27]–[29], which has been employed to coordinate the power exchange participants, e.g. the BTBCs and the MG central controllers in BTBC-IMGs. The disadvantages of high-bandwidth central controller such as single point-of-failure and huge data transfer [35], push authors to use the distributed control methods for IMG power exchange [17], [20], [21]. Nevertheless, the emergency power exchange, which needs to be fast, leads to using communication-free local measurement-based power exchange methods [14], [19], [24], [32], [33], especially for small-scale IMGs. By increasing the number of MGs, communicating data is unavoidable due to numerous variables and high level of the complexity. Therefore, the communication-free methods are still limited to emergency power exchange among a low number of IMGs.

### B. Paper Contribution and Features

In this paper, an emergency-based IMG formation and cancellation are studied that encounters the challenges of emergency situation and its elimination detection, as well as power sharing between IMGs. The main contribution and notable features of this paper are as follows:

- A completely automatic detection of emergency condition and its stop are proposed using local measurement and without employing communication links. All BTBC control processes are based on this detection that means an emergency IMG power exchange. In addition, the lack of using communication links enhances the reliability.
- In contrast with the existing works [17], [24], [28], both voltage and frequency deviations of individual MGs are sensed to detect the emergency condition. It is obvious that in individual MGs, the voltage and frequency deviations in association with the active and reactive powers are related to the X/R ratio of DGs coupling line

This article has been accepted for publication in a future issue of this journal, but has not been fully edited. Content may change prior to final publication. Citation information: DOI 10.1109/JESTPE.2019.2954113, IEEE Journal of Emerging and Selected Topics in Power Electronics

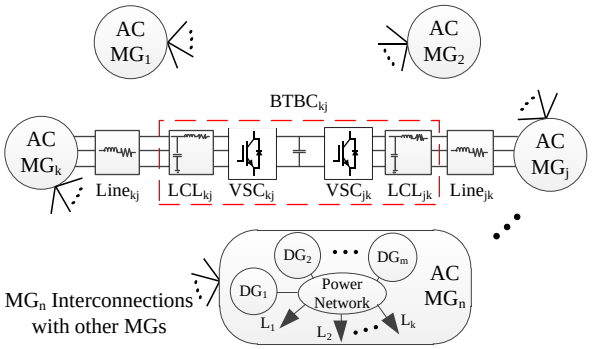


Fig. 1. A general structure of interconnected AC microgrids through back-to-back converters and AC lines focusing on interconnection between $MG_k$ and $MG_j$ by $BTBC_{kj}$.

impedances. Therefore, in MGs with different X/R ratios, the voltage and frequency deviations can have different situations. An emergency condition in all these situations should be detectable, which is possible only by sensing both voltage and frequency of individual MGs.

- The voltage and frequency differences of BTBC's AC sides are a complete set to determine the value of active and reactive powers to be exchanged. This set is applied to a generalized droop control (GDC) method to produce the power references for the interlinking BTBC. The GDC method shares the power robustly between IMGs against the interlinking line X/R ratio. In addition, the GDC produces the active and reactive power references separately by decoupling the interferences of the voltage and frequency deviations.
- The proposed emergency control is compatible with the primary controllers of both sending and receiving MGs due to considering the rated powers and maximum acceptable voltage and frequency deviations of individual MGs in the GDC and logical control designs.

The rest of this paper is organized as follows. Section II addresses the basis of IMG control including individual MG and interlinking BTBC controls. In Section III, the proposed emergency power exchange control is illustrated. Real-time simulation results and discussions are presented in Section IV. Finally, the paper is concluded in Section V.

## II. Basic Controls of Interconnected Microgrids

A general structure of AC BTBC-IMGs including Individual MGs, interlinking lines and BTBCs is shown in Fig. 1. In this section, the main control structure of such IMGs including Individual MGs and BTBCs is presented.

### A. Individual Microgrid Control

In order to have a stable, reliable and efficient MG operation, many controllers are needed to take the responsibility of all MG control objectives in different operation modes and time scales. Therefore, a hierarchical control strategy is applied, which consists of four levels (three levels in some references e.g. [36]), namely the primary (local), secondary, central/emergency, and global controls [13]. For an islanded MG, voltage and frequency stability, current limiting, and active and reactive power sharing are done in the local control

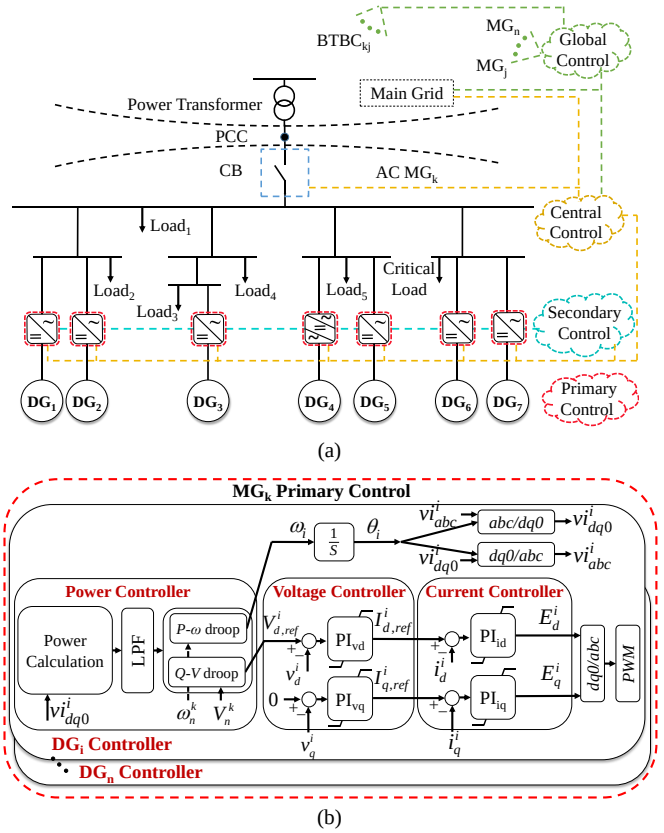


Fig. 2. (a) Hierarchical four-level microgrid control comprising primary, secondary, central and global control levels. (b) Primary control level for the autonomous operation of the typical $MG_k$.

level. The secondary control improves power sharing and restores the deviated voltage and frequency to the nominal values [37], [38]. The central/emergency control level promotes the supervisory MG activities such as grid connecting, islanding detection and emergency control [13]. Finally, the global control plans the optimal power flow between MGs themselves and the main grid [3]. Fig. 2(a) shows a general scheme of the four-level hierarchical control for a typical MG.

A considerable difference between the control levels is their time scale of activation. Basically, the primary control is on-line and acts instantly after events, however the secondary level can have a slower response (a few seconds) to give time to the primary level to complete its action. The upper control levels act in the larger time spans respectively, except some functions such as the emergency control, which has to act as fast as possible in order to avoid instability.

All planned power exchanges between IMGs are managed in the global control. Nevertheless, the emergency power exchange, which is focus of this paper, should be considered as a part of each emergency MG control to support the critical MG. Therefore, the emergency power exchanges among the IMGs should be faster than the secondary control of each individual MG. According to this fact, only the primary controls of individual MGs are considered in this paper.

The primary control consists of the droop characteristics and internal loops, i.e. the current and voltage loops, which are shown in Fig. 2(b). The DG output powers are calculated and filtered as follows

This article has been accepted for publication in a future issue of this journal, but has not been fully edited. Content may change prior to final publication. Citation information: DOI 10.1109/JESTPE.2019.2954113, IEEE Journal of Emerging and Selected Topics in Power Electronics

$$P_i = \frac{\omega_c}{s+\omega_c}(v_d^i i_{od}^i + v_q^i i_{oq}^i), \tag{1a}$$

$$Q_i = \frac{\omega_c}{s+\omega_c}(v_d^i i_{oq}^i - v_q^i i_{od}^i), \tag{1b}$$

where, $\omega_c$ is the cut-off frequency of the low pass filter (LPF), $s$ is the Laplace operator, $v_d^i$, $v_q^i$, $i_{od}^i$, and $i_{oq}^i$ are the direct and quadrature components of the output $\text{DG}_i$ voltage and current, and $P_i$ and $Q_i$ are the averaged active and reactive output powers of $\text{DG}_i$. The $\text{DG}_i$ frequency $\omega_i$ and voltage magnitude reference $V_{d,ref}^i$ are provided using the well-known $\omega - P$ and $v - Q$ droop characteristics as follows

$$\omega_i = \omega_n^k - m_p^i P_i, \tag{2a}$$

$$V_{d,ref}^i = V_n^k - n_q^i Q_i, \tag{2b}$$

where, $\omega_n^k$ and $V_n^k$ are the nominal frequency and voltage amplitude of $\text{MG}_k$. $m_p^i$ and $n_q^i$ are the $\omega - P$ and $v - Q$ droop coefficients of $\text{DG}_i$, which are calculated as follows

$$m_p^i = \Delta\omega_{\max}^k / P_r^i, \tag{3a}$$

$$n_q^i = \Delta V_{\max}^k / Q_r^i, \tag{3b}$$

where, $\Delta\omega_{\max}^k$ and $\Delta V_{\max}^k$ are the maximum acceptable frequency and voltage amplitude deviations in $\text{MG}_k$ and $P_r^i$ and $Q_r^i$ are the rated active and reactive powers of $\text{DG}_i$. The quadrature voltage reference of $\text{DG}_i$, $v_{q,ref}^i$, is usually considered to be zero in order to earn a zero voltage phase angle at phase $a$.

In the voltage control loop, $v_{d,ref}^i$ and $v_{q,ref}^i$ are used to be tracked by the measured voltages using two PI controllers. Similar PI structure is used for converter current control. Main duty of this loop is converter current limiting.

In this paper, the DC links of DGs converters are assumed to be ideal DC voltage sources, i.e. the DGs can provide their ratings during an emergency condition, which cause predetermined voltage/frequency drops due to the droop characteristics. In practice, this assumption is acceptable when the MG can provide enough power by dispatchable DGs.

### *B. Interlinking Back-to-back Converter Control*

As mentioned, the power flow between two IMGs is controlled using a BTBC. Fig. 3 shows the BTBC including two VSCs and their control units. The $\text{VSC}_1$ is controlled as a power flow controller, while the $\text{VSC}_2$ is controlled as a DC voltage controller. The power controller try to flow power between IMGs based on the active and reactive power references and the DC voltage controller stabilizes the DC capacitor voltage during operation. Since the BTBC should be connected to the MGs, two PLLs are required to synchronize VSCs to MGs during power exchange.

The power controller receives the active and reactive power references, $P_{ref}^{C1}$ and $Q_{ref}^{C1}$, from an upper control level. In the case of planned power exchanges, this upper control level is generally the global MG control as shown in Fig. 2(a). On the other hand, in the emergency power exchange, the power references come from the emergency control. In this paper, the power references are produced in an event-based GDC, which is explained in the next section. The active and reactive powers can be exchanged by tracking the references using a PI current controller. The current references, $i_{d,ref}^{C1}$ and $i_{q,ref}^{C1}$, are calculated as [39]

$$i_{d,ref}^{C1} = P_{ref}^{C1}/V_d^{C1}, i_{q,ref}^{C1} = Q_{ref}^{C1}/V_d^{C1}, \tag{4}$$

where, $V_d^{C1}$ is the direct component of the AC side voltage of the $\text{VSC}_1$. Therefore, a PI current controller can be employed to achieve the power control as follows

$$E_d^{C1} = K_{PC1} e_d^{C1} + K_{IC1} \int e_d^{C1} dt - L_f^{C1} \omega_n i_q^{C1} + v_d^{C1}, \tag{5a}$$

$$E_q^{C1} = K_{PC1} e_q^{C1} + K_{IC1} \int e_d^{C1} dt + L_f^{C1} \omega_n i_d^{C1} + v_q^{C1}, \tag{5b}$$

where, $e_{dq}^{C1} = i_{dq,ref}^{C1} - i_{dq}^{C1}$, $i_d^{C1}$ and $i_q^{C1}$ are the measured currents of $\text{VSC}_1$ AC side, $L_f^{C1}$ is the filter inductance of $\text{VSC}_1$, $E_d^{C1}$ and $E_q^{C1}$ are the direct and quadrature components of the $\text{VSC}_1$ output voltage, and $K_{PC1}$ and $K_{IC1}$ are the proportional and integral gains of the $\text{VSC}_1$ current controller. Hence, by applying a control effort on the $\text{VSC}_1$ output voltage as (5), the desired powers expressed in (4) are flowing.

The injected/absorbed power to/from the DC link should be delivered/received to/from the AC side of $\text{VSC}_2$. Otherwise the power cannot be exchanged and the DC voltage will be unstable. Therefore, a similar power control should be applied on $\text{VSC}_2$ with a mandatory active power reference $P_{ref}^{C2} = -P_{ref}^{C1}$ and an optional reactive power reference, $Q_{ref}^{C2}$. In addition, the DC voltage of BTBC should be controlled by the $\text{VSC}_2$ controller. Therefore, another PI controller is employed, which tries to control $V_{dc}$ as follows

$$P_{ref}^{C2} = K_P^{dc}(V_{dc}^{ref} - V_{dc}) + K_I^{dc} \int (V_{dc}^{ref} - V_{dc}) dt - P_{ref}^{C1}. \tag{6}$$

A fully correct operation of the BTBC depends on two other loops including the PLL and initial DC voltage control. Both PLLs should be tuned well in order to ignore their dynamics in the main controllers. Besides, the DC capacitor should be charged to have an initial voltage near the $V_{dc}^{ref}$. This decreases the possibility of instability during the BTBC start up by decreasing the oscillations and overshoot of the $V_{dc}$. The capacitor charger is not included in this study.

## III. Proposed Emergency Power Exchange Control

To benefit from the surplus energy of the adjacent MGs in a critical MG, an emergency control is required to detect the emergency condition. On the other hand, it should be checked whether the adjacent MG has enough energy to exchange without exceeding limitations or not. In such a control process, logical controllers and nonlinear constraints are inevitable.

In the proposed emergency control, both detection of the critical condition in the receiving MG and the excess power in the sending MG are based on the voltage magnitude and frequency monitoring. According to the droop characteristics, an overload, a DG trip, or any change in the MG production/consumption can be seen as voltage, frequency or both deviations. Therefore, the output DG powers or load powers does not need to be measured and communicated in order to detect the emergency/normal condition. Using only the local voltage magnitude and frequency of AC sides of the interlinking BTBC avoids the communication links and facilitates the emergency power exchange.

This article has been accepted for publication in a future issue of this journal, but has not been fully edited. Content may change prior to final publication. Citation information: DOI 10.1109/JESTPE.2019.2954113, IEEE Journal of Emerging and Selected Topics in Power Electronics

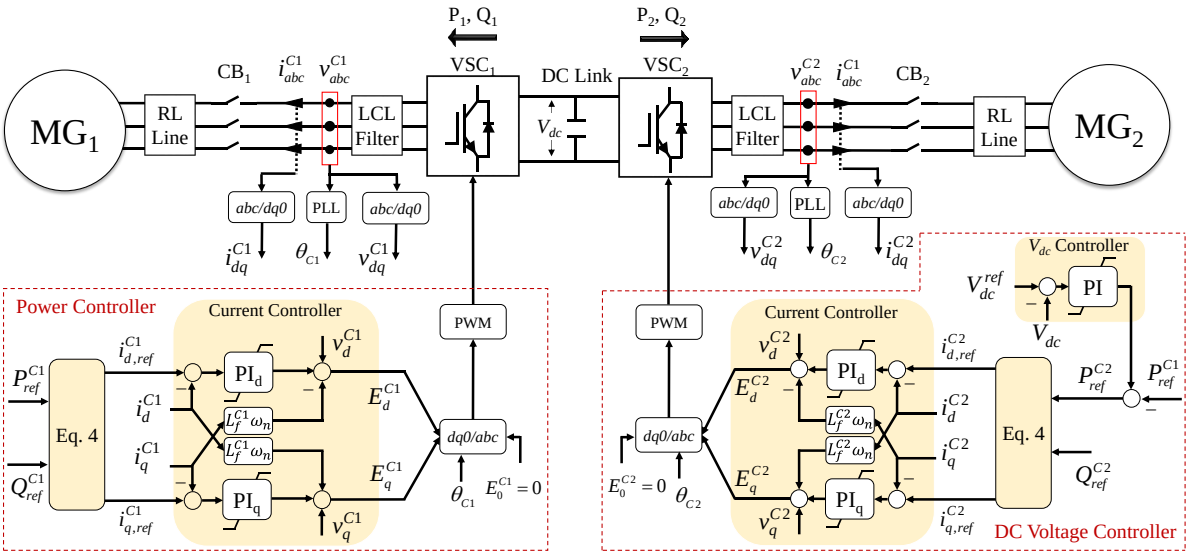


Fig. 3. Basic control of the back-to-back converter including power and DC voltage controllers in order to exchange power between microgrids.

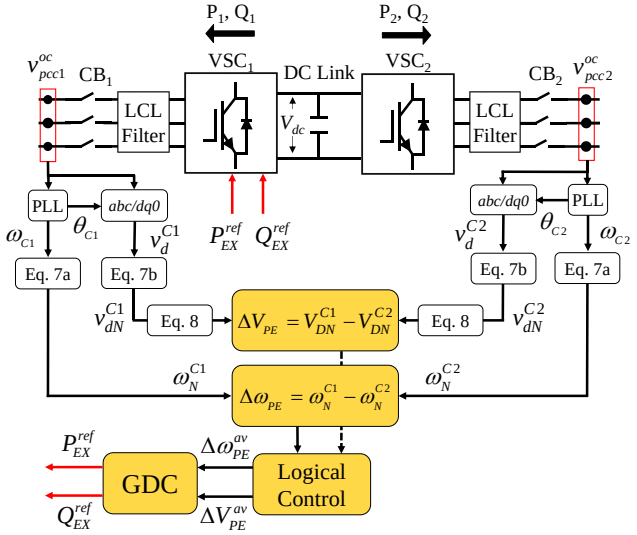


Fig. 4. Overview of the proposed emergency control for power exchange of interconnected microgrids via back-to-back converter.

Fig. 4 shows the schematic of the proposed control framework. The open circuit voltage amplitude and frequency of AC BTBC sides before the CBs are available via voltage sensors and PLLs of the BTBC. These voltages are used in the basic BTBC control in order to synchronize it with both AC sides.

Before using the voltage magnitude and frequency of AC sides in the emergency controller, they should be normalized:

$$\omega_N^{Ci} = \omega_{Ci}/\omega_n^k, \tag{7a}$$
$$v_{dN}^{Ci} = v_d^{Ci}/V_n^k, \tag{7b}$$

where $\omega_{Ci}$ and $v_d^{Ci}$ are the measured frequency and voltage amplitude of VSC$_i$, $\omega_N^{Ci}$ and $v_{dN}^{Ci}$ are the normalized frequency and voltage amplitude and $i = 1, 2$. In addition, the voltage amplitudes should be transformed in a common reference frame, because in practice they are calculated in two different reference frames by the asynchronous PLLs. The transformation is straight-forward as

$$\Delta V_{DQ} = T_s.\Delta v_{dq}, \tag{8}$$

where the $V_{DQ}$ and $v_{dq}$ express variables in common and individual reference frames respectively, and

$$T_s = \begin{bmatrix} \cos\Delta\delta & -\sin\Delta\delta \\ \sin\Delta\delta & \cos\Delta\delta \end{bmatrix},$$

where $\Delta\delta$ is the angle difference between each individual reference frame and the common reference frame. Note that the common reference frame can be selected from each one of individual reference frames of MGs.

The difference between the voltage magnitude and frequency of two AC BTBC sides after the normalization and transformation, $\Delta\omega_{PE}$ and $\Delta V_{PE}$, are provided as follows

$$\Delta\omega_{PE} = \omega_N^{C1} - \omega_N^{C2}, \tag{9a}$$
$$\Delta V_{PE} = V_{DN}^{C1} - V_{DN}^{C2}. \tag{9b}$$

Since $\Delta\omega_{PE}$ and $\Delta V_{PE}$ are the voltage magnitude and frequency differences between a critical MG and a normal MG, they show that how much active and reactive powers should be exchanged between them and when the BTBC should be connected. In fact, by applying $\Delta\omega_{PE}$ and $\Delta V_{PE}$ to a GDC after a necessary logical process, the references of BTBC's active and reactive power exchanges are determined. These powers are injected to the critical MG and lead to frequency/voltage support. In other words, a power shortage in the critical MG is compensated by the adjacent MG reserve flown through the BTBC.

It is noteworthy that in this application of IMGs, the BTBC is connected only during an emergency condition, which can be detected by a logical control. In addition to this function, other functions such as detecting the return to normal condition, disconnecting IMGs and averaging the voltage and frequency deviations are included in the logical controller, which is explained in the later subsection.

### A. Logical Control

Fig. 5 shows the flow-chart of the logical control including emergency condition detection, averaging the deviations and normal condition detection after an event. The $\Delta\omega_{PE}$ and

This article has been accepted for publication in a future issue of this journal, but has not been fully edited. Content may change prior to final publication. Citation information: DOI 10.1109/JESTPE.2019.2954113, IEEE Journal of Emerging and Selected Topics in Power Electronics

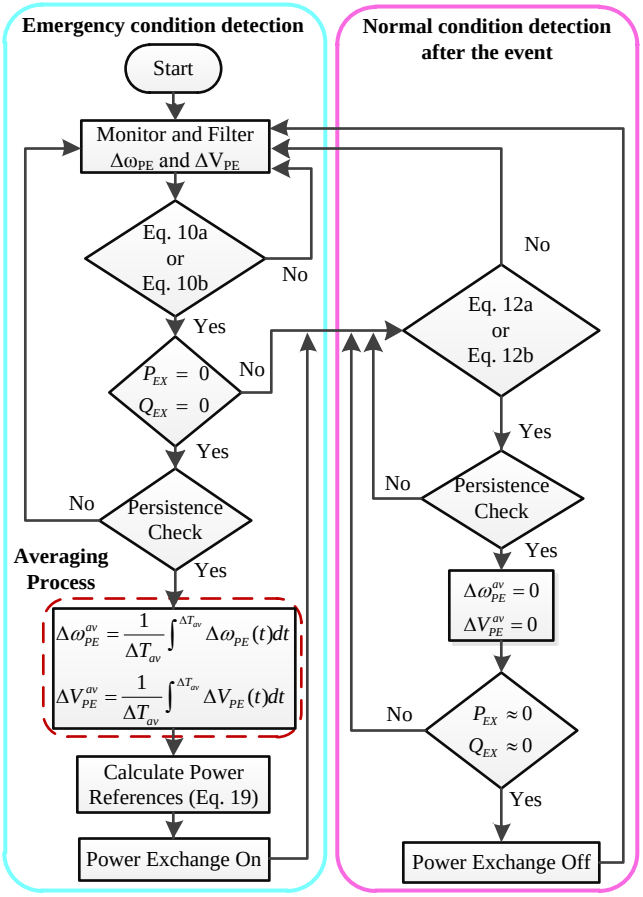


Fig. 5. Flow-chart of the logical control, used in proposed emergency power exchange including detection of emergency and normal conditions.

$\Delta V_{PE}$ are measured continuously as (9) and compared with their thresholds $\Delta\omega_{Tr}^{On}$ and $\Delta V_{Tr}^{On}$ as follows

$$|\Delta\omega_{PE},| > \Delta\omega_{Tr}^{On}, \tag{10a}$$
$$|\Delta V_{PE}| > \Delta V_{Tr}^{On}. \tag{10b}$$

Note that the emergency condition can be detected by each one of (10a) or (10b). The threshold values are defined such that the normal condition is not included and the emergency condition is detected before exceeding the limitations of the individual receiving MG as follows

$$\left|\Delta\omega_{NC,\max}^{MG}\right| < \Delta\omega_{Tr}^{On} < \left|\Delta\omega_{\max}^{k}\right|, \tag{11a}$$
$$\left|\Delta V_{NC,\max}^{MG}\right| < \Delta V_{Tr}^{On} < \left|\Delta V_{\max}^{k}\right|, \tag{11b}$$

where, $\Delta\omega_{\max}^{k}$ and $\Delta V_{\max}^{k}$ are related to MG$_k$ power controllers through (3a) and (3b), and can be calculated as $0.5\%$ of the nominal frequency and $10\%$ of the nominal voltage amplitude [40]. $\Delta\omega_{NC,max}^{MG}$ and $\Delta V_{NC,max}^{MG}$ are the design parameters such that the larger amounts result in more strict detection and vice versa. Another condition for the emergency detection is that the BTBC is off i.e. $P_{EX} = 0$ and $Q_{EX} = 0$. In order to avoid the detection during transient voltage/frequency changes, in addition to use an LPF, a persistence check is included.

Once $\Delta\omega_{PE}$ and $\Delta V_{PE}$ start to go to zero after the emergency power exchange from the normal MG to the critical MG, their related $P_{EX}^{ref}$ and $Q_{EX}^{ref}$ deviate unintentionally from

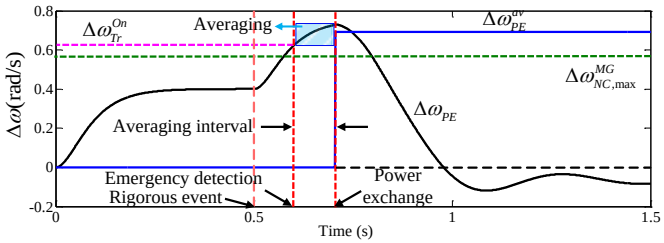


Fig. 6. Detecting, averaging and fixing processes of the frequency deviation after an emergency condition.

the desired amounts. This is due to the lack of an integrator in the GDC method, which causes an oscillating power exchange. In order to avoid these oscillations and stabilize the power references during the power exchange, $\Delta\omega_{PE}$ and $\Delta V_{PE}$ are averaged and frozen on the averaging values, i.e. $\Delta\omega_{PE}^{av}$ and $\Delta V_{PE}^{av}$ before exchanging the power. Fig. 6 shows the averaging procedure after a rigorous event and its detection in the case of $\Delta\omega_{PE}$. If a persistent increase in the $\Delta\omega_{PE}$ or $\Delta V_{PE}$ compared to their thresholds occurs, the averaging is started and the amount is fixed after the averaging interval $\Delta T_{av}$. The averaging interval is another design parameter such that the larger averaging interval leads to the slower detection, which results in the more precise averaging for small disturbances and causes poor averaging or even instability in the large disturbances. In fact, it is a trade-off between the averaging accuracy and detection quickness.

The last function, considered in the logical control, is detecting the normal condition after the event. A special constraint to not mixed up with the emergency detection is considered as follows

$$|\Delta\omega_{PE} + \Delta\omega_{PE}^{av}| < \Delta\omega_{Tr}^{Off}, \tag{12a}$$
$$|\Delta V_{PE} + \Delta V_{PE}^{av}| < \Delta V_{Tr}^{Off}, \tag{12b}$$

where, $\Delta\omega_{Tr}^{Off}$ and $\Delta V_{Tr}^{Off}$ are the thresholds of the frequency and voltage magnitude deviations for stopping the power exchange. The normal condition can be detected by each one of (12a) or (12b).

The thresholds should be theoretically zero and (12a) and (12b) should be in equality form. Nevertheless, in the practical cases, the equality conditions are hardly satisfied. Therefore, the $\Delta\omega_{Tr}^{Off}$ and $\Delta V_{Tr}^{Off}$ are considered less than $10\%$ of $\Delta\omega_{Tr}^{On}$ and $\Delta V_{Tr}^{On}$, respectively. The compulsory constraint before stopping the power exchange completely by opening the CB, is decreasing the exchanging power to zero. This condition is included in the logical controller as $P_{EX} \approx 0$ and $Q_{EX} \approx 0$, which can be seen in Fig. 5. A persistence check is included in this function.

### *B. Generalized Droop Control*

The GDC power sharing method provides an opportunity to exchange the active and reactive powers according to the both frequency and voltage deviations. The benefit of GDC is more obvious when X/R ratio of the MGs is taken into account. As an example, one can consider an AC MG, which $X/R < 1$ or $X/R \simeq 1$ for DG coupling lines. It is obvious that the active load changes lead to larger voltage deviation than the

This article has been accepted for publication in a future issue of this journal, but has not been fully edited. Content may change prior to final publication. Citation information: DOI 10.1109/JESTPE.2019.2954113, IEEE Journal of Emerging and Selected Topics in Power Electronics

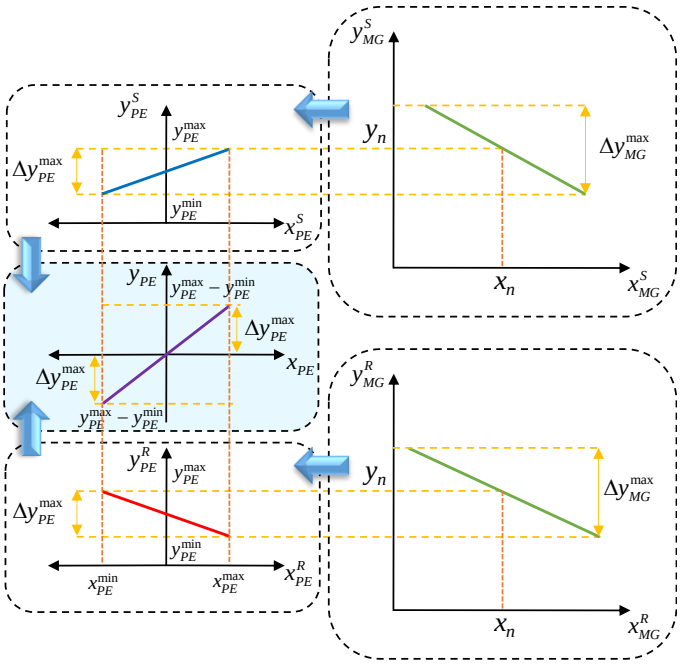


Fig. 7. Relationship between different droop characteristics used in calculating gains of the proposed GDC method including main MG droops, power exchange MG droops and proposed GDC-based droop.

frequency deviation for the normalized variables [41]. In such a case, only measuring the frequency is not enough because it is stable and the critical voltage amplitude, which is not measured will be the reason for the instability.

As mentioned, the $\Delta\omega^{av}_{PE}$ and $\Delta V^{av}_{PE}$ determine the references of the exchanged active and reactive powers. For this purpose, the droop characteristics can be employed. As the AC interlinking lines may have different lengths, in order to decouple the active and reactive powers, a GDC method is used to separate the impact of $\Delta\omega^{av}_{PE}$ and $\Delta V^{av}_{PE}$ on the $P^{ref}_{EX}$ and $Q^{ref}_{EX}$, respectively. Therefore, the rotational power references as ancillary variables [41], [42], are obtained as

$$P'^{ref}_{EX} = \frac{X_{IL}}{Z_{IL}}\left[P^0_{EX} - \frac{\Delta\omega^{av}_{PE}}{k_p}\right] + \frac{R_{IL}}{Z_{IL}}\left[\frac{\Delta V^{av}_{PE}}{k_p} - Q^0_{EX}\right],$$
$$Q'^{ref}_{EX} = \frac{R_{IL}}{Z_{IL}}\left[P^0_{EX} - \frac{\Delta\omega^{av}_{PE}}{k_p}\right] + \frac{X_{IL}}{Z_{IL}}\left[Q^0_{EX} - \frac{\Delta V^{av}_{PE}}{k_p}\right], \quad (13)$$

where, $R_{IL}$, $X_{IL}$ and $Z_{IL}$ are the resistance, inductance and impedance of the interlinking line, and $P^0_{EX}$ and $Q^0_{EX}$ are the nominal active and reactive exchanged powers. $k_p$ and $k_q$ are the coefficients of the conventional droop characteristics in the case of power exchange i.e. $\Delta\omega_{PE} - P_{EX}$ and $\Delta V_{PE} - Q_{EX}$. Two main points should be considered to find the coefficients:

1) The frequency and voltage magnitude of each MG should not be exceeded due to exchanging the power. This can be satisfied by limiting $\Delta\omega^{max}_{PE}$ and $\Delta V^{max}_{PE}$ to the maximum deviations of the same variables from their nominal values in both sending and receiving MGs. Fig. 7 shows the relationship between the droop characteristics of the receiving MG ($y^R_{MG} - x^R_{MG}$), its power exchange ($y^R_{PE} - x^R_{PE}$), sending MG ($y^S_{MG} - x^S_{MG}$), its power exchange ($y^S_{PE} - x^S_{PE}$) and the proposed GDC-based emergency controller ($\Delta y_{PE} - x_{PE}$). Note that the power exchange droops are related to the VSCs of the BTBC. Without loss of generality and in order to show clearer graphs, $MG_1$ and $MG_2$ are considered as sending and receiving MGs respectively and the same nominal values are considered for both MGs. Besides, the output power ($x$) direction is considered in the power direction of $VSC_1$. According to the MG droop characteristics, the maximum $y$ axis deviation of the power exchange droop for each sending/receiving MG, $\Delta y^{max}_{PE}$, is obtained as follows

$$\Delta y^{max}_{PE} = (1/2).\Delta y^{max}_{MG}, \quad (14)$$

where, $y \in \begin{bmatrix} \omega & V \end{bmatrix}^T$ for $x \in \begin{bmatrix} P & Q \end{bmatrix}^T$, respectively. $\Delta y^{max}_{MG}$ equals $\Delta\omega^k_{max}$ or $\Delta V^k_{max}$ of $MG_k$. This constraint limits the sender MG to send power only for situations that there is enough power equivalent to utmost $(1/2).\Delta y^{max}_{MG}$.

2) According to (9), the proposed GDC-based droop characteristic is a subtraction of the power exchange droop characteristics of sending and receiving MGs as

$$\Delta y_{PE} = y^S_{PE} - y^R_{PE}. \quad (15)$$

Hence, the $k_p$ and $k_q$ are calculated according to the frequency and voltage limitations and maximum powers of GDC-based droop characteristics (15) as follows

$$k_p = \frac{(\omega^{max}_{PE} - \omega^{min}_{PE}) - (\omega^{min}_{PE} - \omega^{max}_{PE})}{P^{max}_{PE} - (-P^{max}_{PE})} = \frac{\Delta\omega^{max}_{PE}}{P^{max}_{PE}}, \quad (16a)$$
$$k_q = \frac{(V^{max}_{PE} - V^{min}_{PE}) - (V^{min}_{PE} - V^{max}_{PE})}{Q^{max}_{PE} - (-Q^{max}_{PE})} = \frac{\Delta V^{max}_{PE}}{Q^{max}_{PE}}, \quad (16b)$$

where $\Delta\omega^{max}_{PE}$ and $\Delta\omega^{max}_{PE}$ are calculated using (14), and $P^{max}_{PE}$ and $Q^{max}_{PE}$ are the rated active and reactive powers of the interlinking BTBC determined as

$$x^{max}_{PE} = (1/2).x^{max}_{MGs}, \quad (17)$$

where $x^{max}_{MGs}$ is the active/reactive power of the sender MG, which can be recognized by the frequency/voltage deviation sign according to (9). This constraint limits the rated $BTBC_{ij}$ power between $MG_i$ and $MG_j$ as

$$x^{max}_{PEij} = (1/2).max\{x^{max}_{MGi}, x^{max}_{MGj}\}. \quad (18)$$

Finally, the main references of the active and reactive exchanged powers can be calculated as

$$\begin{bmatrix} P^{ref}_{EX} \\ Q^{ref}_{EX} \end{bmatrix} = K_z \begin{bmatrix} X_{IL}/Z_{IL} & R_{IL}/Z_{IL} \\ -R_{IL}/Z_{IL} & X_{IL}/Z_{IL} \end{bmatrix} \begin{bmatrix} P^{ref}_{EX} \\ Q^{ref}_{EX} \end{bmatrix}', \quad (19)$$

where, $K_z = ((R_{IL}/Z_{IL})^2 + (X_{IL}/Z_{IL})^2)^{-1}$. Note that, $P^{ref}_{EX}$ and $Q^{ref}_{EX}$ are used in (4) as the power references.

Note that the surplus power of the sender MG is considered to be provided by the ideal DC links of the DGs. Otherwise, a low-bandwidth communication is required among the DGs and the proposed emergency control to precisely determine $x^{max}_{MGs}$.

### C. Coordination of BTBC Emergency Controls

The proposed emergency control for two BTBC-IMGs can be generalized for more IMGs. A coordination is required among connected BTBCs to each MG, in fact among all BTBCs in IMGs. The coordination is based on the minimum number of interconnecting, which means if the first BTBC/connection compensates the power shortage, the second BTBC/connection should be avoided. It is realized by off-line

This article has been accepted for publication in a future issue of this journal, but has not been fully edited. Content may change prior to final publication. Citation information: DOI 10.1109/JESTPE.2019.2954113, IEEE Journal of Emerging and Selected Topics in Power Electronics

TABLE I. POWER AND CONTROL DATA OF THE INTERCONNECTED MGS

| **Parameters** | **Value** | | | |
|---|---|---|---|---|
| RMS line-line voltage (V) | 400 | | | |
| DC voltage and initial value (V) | 780,750 | | | |
| Nominal frequency (rad/s) | $100\pi$ | | | |
| DC capacitor ($\mu$F) | 1200 | | | |
| **MGs** | $MG_1$ | | $MG_2$, $MG_3$ | |
| MG $P_{max}$ (kW) | 3 | | 3 | |
| MG $Q_{max}$ (kVAr) | 1.5 | | 1.5 | |
| Initial load | $0.5P_{max}$ $0.3Q_{max}$ | | $0.8P_{max}$ $0.4Q_{max}$ | |
| **DGs** | $DG_1$ | $DG_2$ | $DG_1$ | $DG_2$ |
| DG ratings ($S_{max}$) (kVA) | 1.12 | 2.24 | 1.12 | 2.24 |
| Series filter inductance (mH) | 1.8 | 1.8 | 1.5 | 1.5 |
| Series filter resistance ($\Omega$) | 0.05 | 0.05 | 0.05 | 0.05 |
| Shunt filter capacitance ($\mu F$) | 3.7 | 7.5 | 5.2 | 10 |
| P-f droop coefficients ($10^{-3}$rad/s.W) | 1.6 | 0.8 | 1.6 | 0.8 |
| Q-V droop coefficients ($10^{-2}$V/VAR) | 6.5 | 3.2 | 6.5 | 3.2 |
| **Basic control coefficients** | $K_P$ | | $K_I$ | |
| PI voltage controller for all DGs | 0.05 | | 20 | |
| PI current controller | 30 | | 500 | |
| PI DC voltage controller | 5 | | 1778 | |
| **Proposed emergency control** | $BTBC_{12}$ | | $BTBC_{13}$ | |
| Emergency detection thresholds | 0.63 rad/s, 13 V | | 0.75 rad/s, 17 V | |
| Normal detection thresholds | 0.35 rad/s, 7 V | | 0.35 rad/s, 7 V | |
| Averaging time interval (s) | 0.1 | | 0.2 | |

adjusting for frequency and voltage thresholds of BTBCs as well as averaging intervals as follows:

$$\Delta\omega_{Tr1}^{On} < \Delta\omega_{Tr2}^{On} < \cdots < \Delta\omega_{Trk}^{On} < \cdots < \Delta\omega_{Trn}^{On}, \quad (20a)$$

$$\Delta V_{Tr1}^{On} < \Delta V_{Tr2}^{On} < \cdots < \Delta V_{Trk}^{On} < \cdots < \Delta V_{Trn}^{On}, \quad (20b)$$

$$\Delta T_{av1} < \Delta T_{av} < \cdots < \Delta T_{avk} < \cdots < \Delta T_{Trn}^{On}, \quad (20c)$$

where $\Delta\omega_{Trk}^{On}$, $\Delta V_{Trk}^{On}$ and $\Delta T_{avk}$ are respectively the frequency threshold, the voltage threshold and the averaging interval of $k$'th priority in MG interconnecting to the critical MG. Hence, after detecting the emergency condition by $BTBC_k$, $BTBC_{k+1}$ has a delay based on the threshold difference, averaging interval difference and persistence check. If $BTBC_{k+1}$ thresholds are also exceeded, it will be connected due to a large power deficiency. Note that more reliable and flexible coordination can be achieved using the communication infrastructure [17], [21], which is leaved for future works.

## IV. REAL-TIME SIMULATION RESULTS

In order to verify the proposed emergency power exchange control, the presented structure in Fig. 8 is implemented in MATLAB/SimPowerSystems. A real-time simulation is provided using OPAL-RT digital simulator OP5600 to indicate a larger degree of practicality for the proposed controller. Fig. 9(a) shows the real-time simulation setup including a host PC, the OPAL-RT target and a LAN cable for networking. Fig. 9(b) shows the conceptual diagram of the real-time simulation process. RT-LAB software version 11.2.1.91 is used as the interface between MATLAB and OPAL-RT simulator. The MATLAB/SimPowerSystems model is loaded on the OPAL-RT through the RT-LAB and the real-time data is come back to the MATLAB environment conversely. Note that the model should be at least split into two subsystems, i.e. a subsystem including all permanent power and control parts

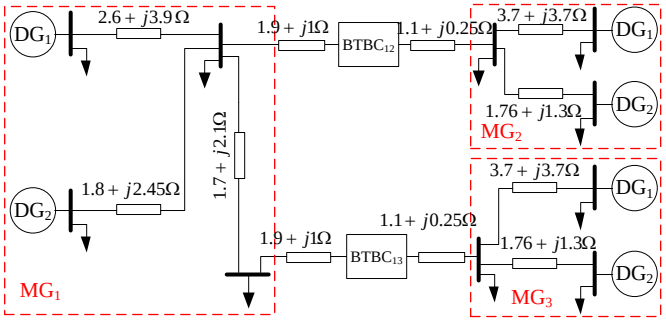


Fig. 8. Study structure of interconnected microgrids including three autonomous microgrids and two back-to-back converters.

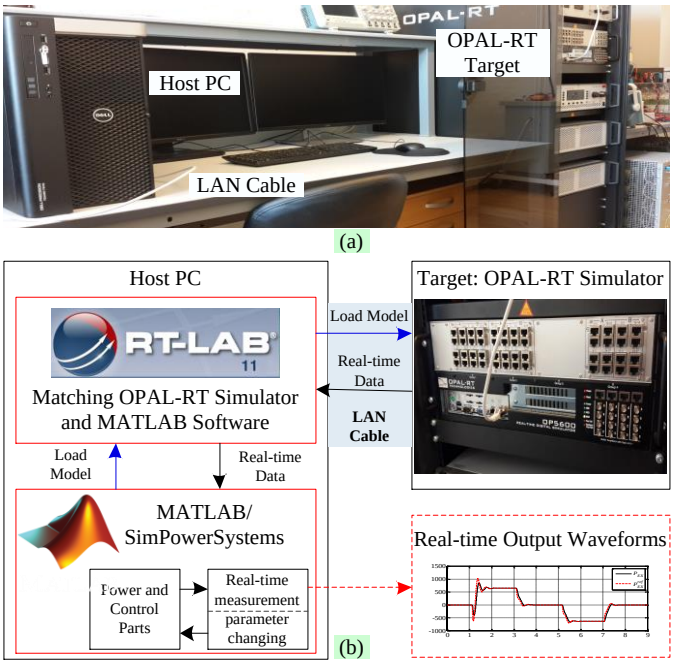


Fig. 9. (a) Real-time simulation setup including the host PC, the OPAL-RT target and a LAN cable for networking. (b) Conceptual diagram of the real-time simulation process.

during the real-time simulation and a subsystem including real-time displays and changeable parameters.

The details of the BTBCs shown in Fig. 8 can be seen in Fig. 3. Each MG has two DGs with the primary control shown in Fig. 2(b). Table I depicts the system information including the power parts and controllers. In Scenarios A-C, only $MG_1$ and $MG_2$ interconnected through $BTBC_{12}$ are studied, but Scenario D includes all three MGs.

### A. Bidirectional Power Flow Support

In this scenario, $MG_1$ and $MG_2$ are operated independently at the beginning until $t = 1$ s. $MG_2$ is overloaded at $t = 1$ s to $1.1P_{\max}^{MG2}$ and $0.6Q_{\max}^{MG2}$ and it comes back to the normal situation at $t = 3$ s. Another rigorous event occurs at $t = 5$ s, which is an $MG_1$ overload as $1P_{\max}^{MG1}$ and $1.1Q_{\max}^{MG1}$. The normal condition after the event is provided at $t = 7$ s.

As shown in Table I, $\Delta\omega_{Tr}^{ON} = 0.63$ rad/s and $\Delta V_{Tr}^{ON} = 13$ V for $BTBC_{12}$, which lead to detecting the emergency condition at $t = 1.04$ s based on the process shown in Fig. 6. Fig. 10 shows the active and reactive exchanging powers at the side of $VSC_2$. According to $\Delta T_{av} = 0.1$ s, the power starts to flow at $t = 1.14$ s from $MG_1$ to $MG_2$ to compensate

This article has been accepted for publication in a future issue of this journal, but has not been fully edited. Content may change prior to final publication. Citation information: DOI 10.1109/JESTPE.2019.2954113, IEEE Journal of Emerging and Selected Topics in Power Electronics

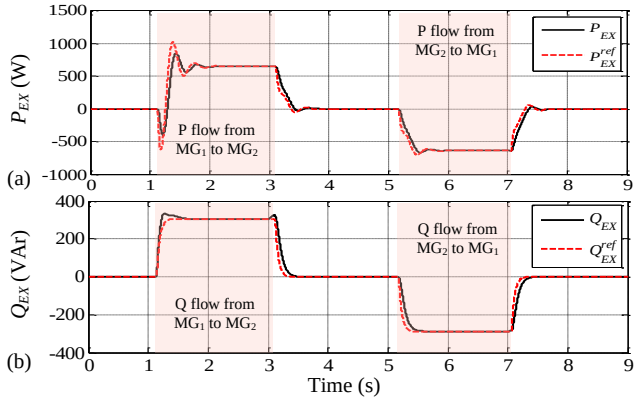


Fig. 10. Exchanging powers from VSC$_2$ side: (a) active, (b) reactive powers.

the MG$_2$ overload. The steady state values of exchanged powers are $P_{EX} = +650$ W and $Q_{EX} = +308$ VAr, which shows the compensation based on the both frequency and voltage amplitude deviations and using (13) in the proposed emergency control. After the overload elimination in MG$_2$ at $t = 3$ s, the normal condition after the event is detected at $t = 3.12$ s and the emergency power exchange is stopped completely at $t = 4$ s by opening the CBs based on the automatic controller command. The second event is detected and the power is exchanged at $t = 5.18$ s. In this emergency situation, only $\Delta V_{PE}$ exceeds its threshold and activates both voltage and frequency averaging process based on the logical control shown in Fig. 5. The emergency controller exchanges $Q_{EX} = +640$ W and $Q_{EX} = +290$ VAr from MG$_2$ to MG$_1$. The clearance is detected at $t = 7.06$ s and the BTBC and MGs are separated completely at $t = 7.67$ s.

Figs. 11(a) and 11(b) show the frequency of the DGs and the PCC voltage of the MGs. The frequency and voltage of MG$_2$ are supported in [1 3] s as well as MG$_1$ frequency and voltage are supported in [5 7] s. The transients of power flow from MG$_1$ to MG$_2$ is larger than the transients of power flow from MG$_2$ to MG$_1$ due to two reasons. 1) The initial DC voltage of the BTBC$_{12}$ at $t = 1$ s is considered to be 750 V. As shown in Fig. 11(c), the $V_{dc}$ increases to the $V_{dc}^{ref} = 780$ V during power flow by charging DC capacitor fully. It is 779.4 V at $t = 5$ s due to the partial discharge. The larger difference between $V_{dc}$ and $V_{dc}^{ref}$ causes larger transients. 2) In the first case, the power flows in the opposite direction of the charging capacitor power. However, they have same direction in the second case, which leads to more smooth transients, lower voltage drop and lower frequency nadir.

Fig. 12 depicts the power sharing and the power support by the proposed emergency controller from the normal MG to the overloaded MG. Both active and reactive power exchanges based on the GDC method improve voltage and frequency controls, which in turn enhance IMG power sharing.

### *B. Comparison Between the Proposed Emergency Control and Multi-frequency Control*

The multi-frequency control has been presented in [28] as a primary coordination of the hierarchical control for a community MG with both AC and DC MGs. Such a control strategy is developed for BTBC-IMGs in [24]. In this method,

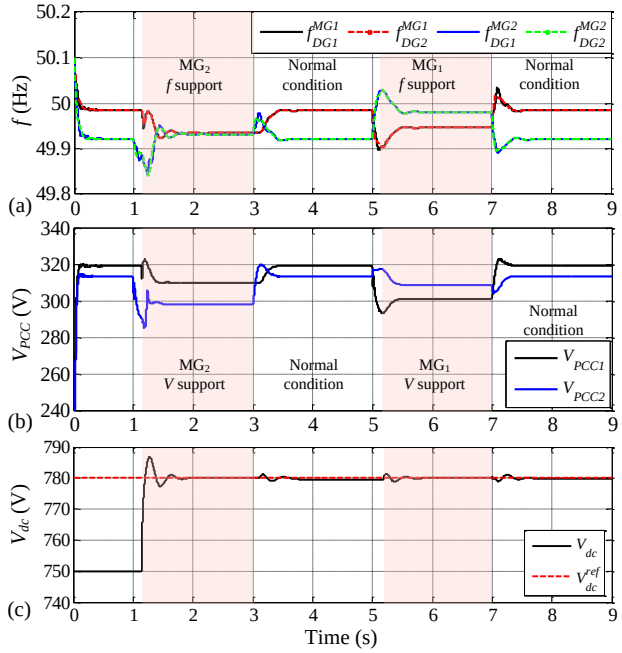


Fig. 11. Interconnected MG features during critical condition under proposed control performance: (a) DG frequencies, (b) MG PCC voltage amplitudes, (c) DC link voltage of BTBC$_{12}$.

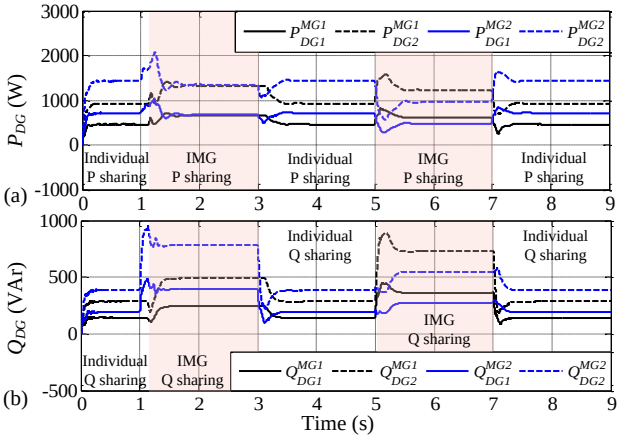


Fig. 12. Power sharing of DGs during emergency and normal conditions: (a) active power sharing, (b) reactive power sharing.

the frequencies of both BTBC sides are measured, and then normalized as follows

$$\omega_N^{Ci} = \begin{cases} \frac{\omega_i - \omega_n^i}{\omega_{\max}^i - \omega_n^i}, & \omega_i > \omega_n^i \quad i = 1,2 \\ \frac{\omega_i - \omega_n^i}{\omega_n^i - \omega_{\min}^i}, & \omega_i < \omega_n^i \quad i = 1,2 \end{cases} \tag{21}$$

where $\omega_{\max}^i$ and $\omega_{\min}^i$ are the maximum and minimum acceptable values of the VSC$_i$ side frequency, $i = 1, 2$. Fig. 13 shows the multi-frequency control method, where the active power reference is obtained based on the difference of the normalized frequencies and using a PI controller. In this method, the voltage amplitude is not used in the power exchange procedure and the reactive power reference for emergency exchanges is zero. However, in planned power exchanges, both active and reactive power references are provided by the global controller.

Consider the MG$_2$ overload at $t = 1$ s mentioned in Section IV-A to compare the proposed emergency control and the

This article has been accepted for publication in a future issue of this journal, but has not been fully edited. Content may change prior to final publication. Citation information: DOI 10.1109/JESTPE.2019.2954113, IEEE Journal of Emerging and Selected Topics in Power Electronics

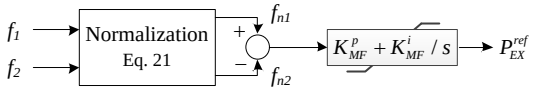


Fig. 13. Active power reference generation in multi-frequency control of interconnected MGs [24], [28].

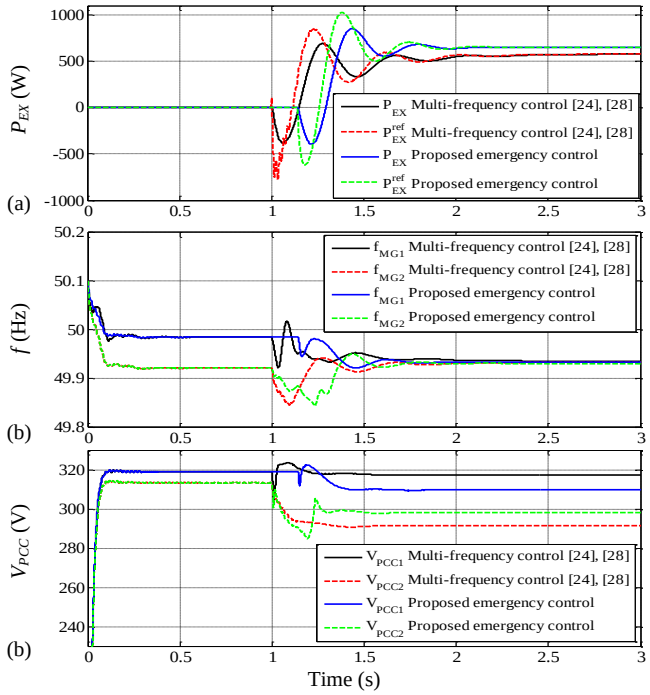


Fig. 14. Comparison between the multi-frequency control in [24], [28] and the proposed emergency control: (a) real and reference active powers, (b) MG frequencies, and (c) MG PCC voltage amplitudes.

multi-frequency control [24], [28]. Since the multi-frequency control has just been used for planned power exchanges, it has no emergency detection. Therefore, a manual start at $t = 1$ s coincided with the overload beginning is considered, which is not valuable in the comparison. Moreover, it is assumed that $\omega^i_{\max} = 1.005\omega^i_n$, $\omega^i_{\min} = 0.995\omega^i_n$ for $i = 1, 2$, $K^p_{MF} = 160$, and $K^i_{MF} = 796$.

Fig. 14(a) shows the active power exchange, where the proposed emergency control provides more active power for $MG_2$ as 50 W. Note that the reactive power reference in the multi-frequency method is zero and cannot participate in the frequency/voltage support except in the transients. Nevertheless, in the proposed emergency method, the reactive power is employed to improve the overloaded MG features as shown in Figs. 10 and 11. As Fig. 14(b) shows, the frequency support is similar in both methods due to the similar use of both BTBC sides frequencies. However, the voltage support of the proposed emergency control is better due to a larger PCC voltage $V_{PCC2} = 298$ V with respect to the PCC voltage in the multi-frequency method ($V_{PCC2} = 291$ V).

### C. Averaging Interval Impact on the Controller Performance

In this scenario, three values are considered for the averaging time interval including 0.05 s, 0.1 s and 0.2 s. The frequency and PCC voltage of MGs are shown in Fig. 15 for same condition with Section IV-A except $V_{dc0} = 780$ V. Since the effect of $\Delta T_{av}$ is only on the activation of the

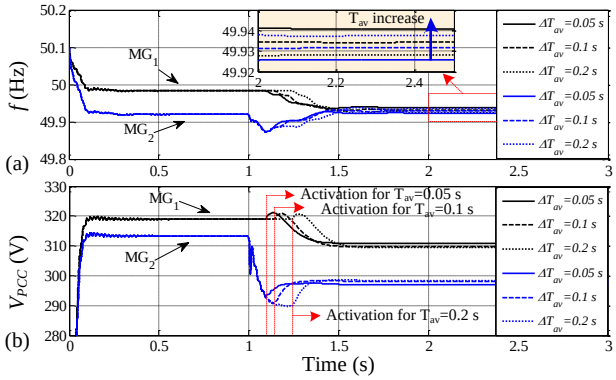


Fig. 15. MG features for different values of the averaging time interval comprising 0.05 s, 0.1 s and 0.2 s: (a) MG frequency, (b) PCC voltage.

proposed emergency control, the normal condition detection and IMG disconnecting are not shown. The larger $\Delta T_{av}$, which gives more time to averaging process results in a better frequency/voltage restoration. Both Figs. 15(a) and 15(b) indicate better restoration (steady state) for $\Delta T_{av} = 0.2$ s. Nevertheless, the larger $\Delta T_{av}$ causes more delay in emergency power flow activating, which may lead to trip of protection devices. The delay can just be seen for the voltage in Fig. 15(b). Because, the frequency does not exceed (10a) and is not challenging for the detection.

### D. DG plug-and-play

A well-known large disturbance in MGs is DG plug-and-play, which leads to power deficiency and can be supported by the proposed emergency controller. It is notable to mention that the secondary control and a synchronization method are necessary for reconnecting the DG. The distributed secondary control and the synchronization method presented in [37] and [43] are used here. $DG_1$ of $MG_1$ is disconnected at $t = 1$ s and it is reconnected at $t = 3$ s. The synchronization method is activated before $t = 3$ s and the secondary control is activated after it. The emergency and normal conditions are detected by the proposed controller at $t = 1.07$ s and $t = 3.07$ s, respectively. Figs. 16(a)-16(d) show $MG_2$ support during the plug-and-play. The secondary control in $MG_1$ leads to frequency and voltage restoration as well as different power sharing, especially in the case of reactive power.

### E. Three Interconnected Microgrids

In this scenario, all three MGs are considered to validate coordination process between individual emergency controllers of $BTBC_{12}$ and $BTBC_{13}$. The thresholds of $BTBC_{12}$ is lesser as shown in Table I. As shown in Fig. 17, $MG_1$ is overloaded at $t = 1$ s and it is quickly supported by $MG_2$ due to the lesser thresholds and enough spinning reserve. $MG_1$ comes back to the normal condition at $t = 2$ s and $MG_2$ loses the spare power due to a local full load condition at $t = 3$ s. Next similar $MG_1$ overload condition at $t = 4$ s is not supported by $MG_2$ and $BTBC_{12}$ emergency control due to lack of spare power. However, $MG_3$ and $BTBC_{13}$ compensate the $MG_1$ overload with a larger delay due to the larger thresholds and the larger averaging interval. Finally, $MG_1$ comes back to the normal condition at $t = 6$ s and it is detected well.

This article has been accepted for publication in a future issue of this journal, but has not been fully edited. Content may change prior to final publication. Citation information: DOI 10.1109/JESTPE.2019.2954113, IEEE Journal of Emerging and Selected Topics in Power Electronics

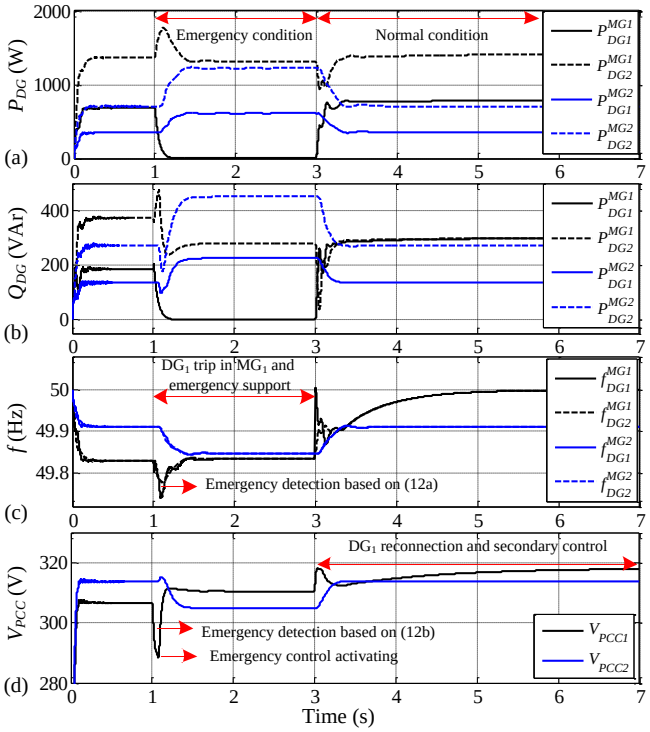


Fig. 16. DG$_1$ plug-and-play scenario in MG$_1$ at $t = 1$ s and $t = 3$ s, respectively: (a) active power, (b) reactive power, (c) frequency, and (d) PCC voltage of MGs.

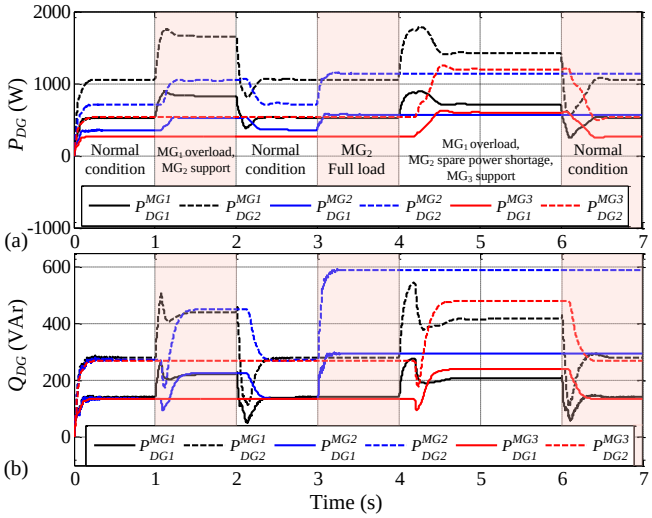


Fig. 17. MG$_1$ power shortage support by MG$_2$ in [1 2] s and MG$_3$ in [4 6] s under emergency control coordination: (a) active power of MGs, (b) reactive power of MGs.

## V. Conclusion

In this paper, a new power exchange control method is employed for interconnected microgrids to overcome the emergency condition in the critical microgrids. In the proposed method, the active and reactive powers are exchanged through the back-to-back converter, based on the voltage magnitude and/or frequency deviations of the individual microgrids. The generalized droop method transforms the frequency and voltage amplitude to the active and reactive powers independently in order to prevent interference between their sharing. The communication challenges are eliminated by using only the local measurements and control. Therefore, the individual microgrids can be interlinked to exchange power based on local measurement of the back-to-back converter. The logical control provides the detection of the emergency condition and also the normal condition after the critical situation. The proposed emergency control is generalized for more microgrids by coordinating emergency controllers of all back-to-back converters. Real-time simulation results show the fast emergency/normal detection and appropriate power exchange/sharing between interconnected microgrids during the emergency condition.

## References

[1] R. H. Lasseter, "Smart distribution: Coupled microgrids," *Proceedings of the IEEE*, vol. 99, no. 6, pp. 1074–1082, 2011.

[2] M. Shahidehpour, Z. Li, S. Bahramirad, Z. Li, and W. Tian, "Networked microgrids: Exploring the possibilities of the iit-bronzeville grid," *IEEE Power and Energy Mag.*, vol. 15, no. 4, pp. 63–71, 2017.

[3] M. Fathi and H. Bevrani, "Statistical cooperative power dispatching in interconnected microgrids," *IEEE Trans. Sustainable Energy*, vol. 4, no. 3, pp. 586–593, 2013.

[4] H. Wang and J. Huang, "Incentivizing energy trading for interconnected microgrids," *IEEE Trans. Smart Grid*, vol. 9, no. 4, pp. 2647–2657, 2018.

[5] B. Zhang, Q. Li, L. Wang, and W. Feng, "Robust optimization for energy transactions in multi-microgrids under uncertainty," *Applied Energy*, vol. 217, pp. 346–360, 2018.

[6] E. H. Trinklein, G. G. Parker, R. D. Robinett, and W. W. Weaver, "Toward online optimal power flow of a networked dc microgrid system," *IEEE J. Emerging and Sel. Topics in Power Electron.*, vol. 5, no. 3, pp. 949–959, 2017.

[7] W. Liu, W. Gu, Y. Xu, Y. Wang, and K. Zhang, "General distributed secondary control for multi-microgrids with both pq-controlled and droop-controlled distributed generators," *IET Gen., Transm. & Dist.*, vol. 11, no. 3, pp. 707–718, 2017.

[8] Z. Zhao, P. Yang, Y. Wang, Z. Xu, and J. M. Guerrero, "Dynamic characteristics analysis and stabilization of pv-based multiple microgrid clusters," *IEEE Transactions on Smart Grid*, 2017.

[9] X. Wu, Y. Xu, X. Wu, J. He, J. M. Guerrero, C.-C. Liu, K. P. Schneider, and D. T. Ton, "A two-layer distributed control method for islanded networked microgrid systems," *ArXiv preprint arXiv:1810.08367*, 2018.

[10] M. S. Golsorkhi, D. J. Hill, and H. R. Karshenas, "Distributed voltage control and power management of networked microgrids," *IEEE J. Emerging and Sel. Topics Power Electron.*, vol. 6, no. 4, pp. 1892–1902, 2018.

[11] P. Kundur, N. J. Balu, and M. G. Lauby, *Power system stability and control*. McGraw-hill New York, 1994, vol. 7.

[12] H. Bevrani, "Robust power system frequency control," 2014.

[13] H. Bevrani, B. François, and T. Ise, *Microgrid dynamics and control*. John Wiley & Sons, 2017.

[14] E. Pashajavid, A. Ghosh, and F. Zare, "A multimode supervisory control scheme for coupling remote droop-regulated microgrids," *IEEE Trans. Smart Grid*, vol. 9, no. 5, pp. 5381–5392, 2018.

[15] S. A. Arefifar, A.-R. M. Yasser, and T. H. El-Fouly, "Optimum microgrid design for enhancing reliability and supply-security," *IEEE Trans. Smart Grid*, vol. 4, no. 3, pp. 1567–1575, 2013.

[16] E. Bullich-Massagué, F. Díaz-González, M. Aragüés-Peñalba, F. Girbau-Llistuella, P. Olivella-Rosell, and A. Sumper, "Microgrid clustering architectures," *Applied Energy*, vol. 212, pp. 340–361, 2018.

[17] M. J. Hossain, M. A. Mahmud, F. Milano, S. Bacha, and A. Hably, "Design of robust distributed control for interconnected microgrids," *IEEE Trans. Smart Grid*, vol. 7, no. 6, pp. 2724–2735, 2016.

[18] P. Wu, W. Huang, N. Tai, and S. Liang, "A novel design of architecture and control for multiple microgrids with hybrid ac/dc connection," *Applied Energy*, vol. 210, pp. 1002–1016, 2018.

[19] I. U. Nutkani, P. C. Loh, and F. Blaabjerg, "Distributed operation of interlinked ac microgrids with dynamic active and reactive power tuning," *IEEE Trans. Ind. App.*, vol. 49, no. 5, pp. 2188–2196, 2013.

[20] Q. Shafiee, T. Dragičević, J. C. Vasquez, and J. M. Guerrero, "Hierarchical control for multiple dc-microgrids clusters," *IEEE Trans. Energy Conv.*, vol. 29, no. 4, pp. 922–933, 2014.

[21] J. Zhou, H. Zhang, Q. Sun, D. Ma, and B. Huang, "Event-based distributed active power sharing control for interconnected ac and dc microgrids," *IEEE Trans. Smart Grid*, 2017.

[22] P. C. Loh, D. Li, Y. K. Chai, and F. Blaabjerg, "Autonomous operation of hybrid microgrid with ac and dc subgrids," *IEEE Trans. Power Electron.*, vol. 28, no. 5, pp. 2214–2223, 2013.

[23] P. C. Loh, D. Li, Y. k. Chai, and F. Blaabjerg, "Hybrid ac–dc microgrids with energy storages and progressive energy flow tuning," *IEEE Trans. Power Electron.*, vol. 28, no. 4, pp. 1533–1543, 2013.

[24] H.-J. Yoo, T.-T. Nguyen, and H.-M. Kim, "Multi-frequency control in a stand-alone multi-microgrid system using a back-to-back converter," *Energies*, vol. 10, no. 6, p. 822, 2017.

[25] R. Zamora and A. K. Srivastava, "Multi-layer architecture for voltage and frequency control in networked microgrids," *IEEE Trans. Smart Grid*, vol. 9, no. 3, pp. 2076–2085, 2018.

[26] I. P. Nikolakakos, H. H. Zeineldin, M. S. El-Moursi, and N. D. Hatziargyriou, "Stability evaluation of interconnected multi-inverter microgrids through critical clusters," *IEEE Trans. Power Syst.*, vol. 31, no. 4, pp. 3060–3072, 2016.

[27] N. J. Gil and J. P. Lopes, "Hierarchical frequency control scheme for islanded multi-microgrids operation," in *Power Tech., Lausanne*. IEEE, 2007, pp. 473–478.

[28] L. Che, M. Shahidehpour, A. Alabdulwahab, and Y. Al-Turki, "Hierarchical coordination of a community microgrid with ac and dc microgrids," *IEEE Trans. smart grid*, vol. 6, no. 6, pp. 3042–3051, 2015.

[29] F. Shahnia, R. P. Chandrasena, S. Rajakaruna, and A. Ghosh, "Primary control level of parallel distributed energy resources converters in system of multiple interconnected autonomous microgrids within self-healing networks," *IET Gen., Transm. & Dist.*, vol. 8, no. 2, pp. 203–222, 2014.

[30] N. Eghtedarpour and E. Farjah, "Power control and management in a hybrid ac/dc microgrid," *IEEE Trans. Smart Grid*, vol. 5, no. 3, pp. 1494–1505, 2014.

[31] L. Yu, R. Li, and L. Xu, "Parallel operation of diode-rectifier based hvdc link and hvac link for offshore wind power transmission," *J. Eng.*, vol. 2019, no. 18, pp. 4713–4717, 2019.

[32] I. U. Nutkani, P. C. Loh, and F. Blaabjerg, "Power flow control of intertied ac microgrids," *IET Power Electron.*, vol. 6, no. 7, pp. 1329–1338, 2013.

[33] I. U. Nutkani, P. C. Loh, P. Wang, T. K. Jet, and F. Blaabjerg, "Intertied ac–ac microgrids with autonomous power import and export," *Int. J. Electr. Power & Energy Syst.*, vol. 65, pp. 385–393, 2015.

[34] L. Ren, Y. Qin, Y. Li, P. Zhang, B. Wang, P. B. Luh, S. Han, T. Orekan, and T. Gong, "Enabling resilient distributed power sharing in networked microgrids through software defined networking," *Applied Energy*, vol. 210, pp. 1251–1265, 2018.

[35] Q. Shafiee, V. Nasirian, J. C. Vasquez, J. M. Guerrero, and A. Davoudi, "A multi-functional fully distributed control framework for ac microgrids," *IEEE Trans. Smart Grid*, vol. 9, no. 4, pp. 3247–3258, 2016.

[36] J. M. Guerrero, J. C. Vasquez, J. Matas, L. G. De Vicuña, and M. Castilla, "Hierarchical control of droop-controlled ac and dc microgrids—a general approach toward standardization," *IEEE Trans. Ind. Electron.*, vol. 58, no. 1, pp. 158–172, 2011.

[37] Q. Shafiee, J. M. Guerrero, and J. C. Vasquez, "Distributed secondary control for islanded microgrids—a novel approach," *IEEE Transactions on power electronics*, vol. 29, no. 2, pp. 1018–1031, 2014.

[38] Y. Khayat, M. Naderi, Q. Shafiee, Y. Batmani, M. Fathi, J. M. Guerrero, and H. Bevrani, "Decentralized optimal frequency control in autonomous microgrids," *IEEE Transactions on Power Systems*, 2018, DOI: 10.1109/TPWRS.2018.2889671.

[39] A. Yazdani and R. Iravani, *Voltage-sourced converters in power systems: modeling, control, and applications*. John Wiley & Sons, 2010.

[40] "British standard: Voltage characteristics of electricity supplied by public distribution networks," *British Standard*, pp. 1505–1513, 2007.

[41] J. Rocabert, A. Luna, F. Blaabjerg, and P. Rodriguez, "Control of power converters in ac microgrids," *IEEE Trans. Power Electron.*, vol. 27, no. 11, pp. 4734–4749, 2012.

[42] H. Bevrani and S. Shokoohi, "An intelligent droop control for simultaneous voltage and frequency regulation in islanded microgrids," *IEEE Trans. Smart Grid*, vol. 4, no. 3, pp. 1505–1513, 2013.

[43] J. C. Vasquez, J. M. Guerrero, M. Savaghebi, J. Eloy-Garcia, and R. Teodorescu, "Modeling, analysis, and design of stationary-reference-frame droop-controlled parallel three-phase voltage source inverters," *IEEE Transactions on Industrial Electronics*, vol. 60, no. 4, pp. 1271–1280, 2013.


**Mobin Naderi** (S'16) was born in Paveh, Iran. He received the B.Sc. and M.Sc. degrees in Electrical Engineering from Tabriz University, Tabriz, Iran, in 2012 and Iran University of Science and Technology, Tehran, Iran, in 2014. He was a Visiting PhD student with Department of Energy Technology, Aalborg University, Aalborg, Denmark. He is now working toward the Ph.D. degree in the control of power systems at the University of Kurdistan, Iran. His research interests focus on robust control methods, and modeling, stability and control of autonomous and interconnected AC microgrids.

**Yousef Khayat** (S'16) received the B.Sc. degree from Urmia University, Urmia, Iran, and the M.Sc. degree (with Hons.) from Iran University of Science and Technology (IUST), Tehran, Iran, both in Electrical Engineering in 2012 and 2014, respectively. He is working toward the Ph.D. degree in control of power systems at the University of Kurdistan, Iran. He is also currently a Ph.D. Visiting Student with Aalborg University, Aalborg, Denmark. His research interests include Microgrid dynamics and control, robust, predictive and nonlinear control for application of power electronics in distributed systems.

**Qobad Shafiee** (S'13–M'15–SM'17) received PhD degree in electrical engineering from the Department of Energy Technology, Aalborg University (Denmark) in 2014. He is currently an Assistant Professor, Director of International Relations, and the Program Co-Leader of the Smart/Micro Grids Research Center at the University of Kurdistan, Sanandaj, Iran, where he was a lecturer from 2007 to 2011. In 2014, he was a Visiting Scholar with the Electrical Engineering Department, the University of Texas at Arlington, Arlington, TX, USA. He was a Post-Doctoral Fellow with the Department of Energy Technology, Aalborg University in 2015. His current research interests include modeling, energy management, control of power electronics-based systems and microgrids, and model predictive and optimal control of modern power systems.

**Tomislav Dragičević** (S'09-M'13-SM'17) received the M.Sc. and the industrial Ph.D. degrees in Electrical Engineering from the Faculty of Electrical Engineering, Zagreb, Croatia, in 2009 and 2013, respectively. From 2013 until 2016 he has been a Postdoctoral research associate at Aalborg University, Denmark. From March 2016 he is an Associate Professor at Aalborg University, Denmark where he leads an Advanced Control Lab.

He made a guest professor stay at Nottingham University, UK during spring/summer of 2018. His principal field of interest is design and control of microgrids, and application of advanced modeling and control concepts to power electronic systems. He has authored and co-authored more than 180 technical papers (more than 80 of them are published in international journals, mostly IEEE Transactions) in his domain of interest, 8 book chapters and a book in the field.

He serves as Associate Editor in the IEEE TRANSACTIONS ON INDUSTRIAL ELECTRONICS, in IEEE Emerging and Selected Topics in Power Electronics and in IEEE Industrial Electronics Magazine. Dr. Dragičević is a recipient of the Končar prize for the best industrial PhD thesis in Croatia, and a Robert Mayer Energy Conservation award.

This article has been accepted for publication in a future issue of this journal, but has not been fully edited. Content may change prior to final publication. Citation information: DOI 10.1109/JESTPE.2019.2954113, IEEE Journal of Emerging and Selected Topics in Power Electronics

**Frede Blaabjerg** (S'86–M'88–SM'97–F'03) was with ABB-Scandia, Randers, Denmark, from 1987 to 1988. From 1988 to 1992, he got the PhD degree in Electrical Engineering at Aalborg University in 1995. He became an Assistant Professor in 1992, an Associate Professor in 1996, and a Full Professor of power electronics and drives in 1998. From 2017 he became a Villum Investigator. He is honoris causa at University Politehnica Timisoara (UPT), Romania and Tallinn Technical University (TTU) in Estonia.

His current research interests include power electronics and its applications such as in wind turbines, PV systems, reliability, harmonics and adjustable speed drives. He has published more than 600 journal papers in the fields of power electronics and its applications. He is the co-author of four monographs and editor of ten books in power electronics and its applications.

He has received 32 IEEE Prize Paper Awards, the IEEE PELS Distinguished Service Award in 2009, the EPE-PEMC Council Award in 2010, the IEEE William E. Newell Power Electronics Award 2014, the Villum Kann Rasmussen Research Award 2014 and the Global Energy Prize in 2019. He was the Editor-in-Chief of the IEEE TRANSACTIONS ON POWER ELECTRONICS from 2006 to 2012. He has been Distinguished Lecturer for the IEEE Power Electronics Society from 2005 to 2007 and for the IEEE Industry Applications Society from 2010 to 2011 as well as 2017 to 2018. In 2019-2020 he serves a President of IEEE Power Electronics Society. He is Vice-President of the Danish Academy of Technical Sciences too. He is nominated in 2014-2018 by Thomson Reuters to be between the most 250 cited researchers in Engineering in the world.

**Hassan Bevrani** (S'90 - M'04 - SM'08) received PhD degree in electrical engineering from Osaka University (Japan) in 2004. Currently, he is a full professor and the Program Leader of Smart/Micro Grids Research Center (SMGRC) at the University of Kurdistan (UOK). From 2016 to 2019 he was the UOK vice-chancellor for research and technology. Over the years, he has worked as senior research fellow and visiting professor with Osaka University, Kumamoto University (Japan), Queensland University of Technology (Australia), Kyushu Institute of Technology (Japan), Centrale Lille (France), and Technical University of Berlin (Germany). Prof. Bevrani is the author of 6 international books, 15 book chapters, and more than 300 journal/conference papers. His current research interests include smart grid operation and control, power systems stability and optimization, Microgrid dynamics and control, and Intelligent/robust control applications in power electric industry.